Synthesis of Boehmite Hollow Core/Shell and Hollow Microspheres via Sodium Tartrate-Mediated Phase Transformation and Their Enhanced Adsorption Performance in Water Treatment

ARTICLE *in* THE JOURNAL OF PHYSICAL CHEMISTRY C · AUGUST 2009

Impact Factor: 4.77 · DOI: 10.1021/jp904570z

5 AUTHORS, INCLUDING:

Weiquan Cai
Wuhan University of Technology
39 PUBLICATIONS **891** CITATIONS
SEE PROFILE

Jiaguo Yu
Wuhan University of Technology
386 PUBLICATIONS **28,597** CITATIONS
SEE PROFILE

Synthesis of Boehmite Hollow Core/Shell and Hollow Microspheres via Sodium Tartrate-Mediated Phase Transformation and Their Enhanced Adsorption Performance in Water Treatment

Weiquan Cai,[†] Jiaguo Yu,*[,†] Bei Cheng,[†] Bao-Lian Su,[†] and Mietek Jaroniec*[,‡]

State Key Laboratory of Advanced Technology for Material Synthesis and Processing and School of Chemical Engineering, Wuhan University of Technology, Luoshi Road 122#, Wuhan 430070, People's Republic of China, and Department of Chemistry, Kent State University, Kent, Ohio 44242

Received: May 16, 2009; Revised Manuscript Received: June 8, 2009

A variety of boehmite hollow core/shell and hollow microspheres with high adsorption affinity toward organic pollutants in water were prepared via a facile one-pot hydrothermal method using aluminum sulfate as a precursor and urea and sodium tartrate as precipitating and mediating agents, respectively. These microspheres were characterized by powder X-ray diffraction, scanning electron microscopy, transmission electron microscopy, and nitrogen adsorption. In addition, the aforementioned microspheres were examined as potential adsorbents for Congo red and phenol from aqueous solutions. This study shows that the crystallinity, specific surface area, and pore structure of the resulting microspheres can be controlled by varying the concentration of sodium tartrate and reaction time. The reported experiments allowed us to propose the mechanism of formation of hollow core/shell and hollow microspheres, which involves sodium tartrate-mediated phase transformation, followed by a subsequent self-assembly process. Adsorption performance of the boehmite microspheres studied is gradually enhanced with increasing concentration of sodium tartrate. This enhancement is substantial in comparison to the performance of the microspheres prepared without sodium tartrate and commercial boehmite powders, and it is probably due to several factors, such as high specific surface area, large pore volume, proper crystallite size, and unique core/shell morphology and structure of the aforementioned microspheres. Especially, the hollow core/shell microspheres prepared at 0.01 M concentration of sodium tartrate exhibited the best adsorption performance, which can be easily regenerated without any great loss in the adsorption capacity. This study suggests that the degree of chemical self-transformation of amorphous particles into crystalline shells, followed by their self-assembly into complex higher-order architectures with desirable functionality, can be mediated by simple organic anions.

1. Introduction

In the past decade, the design and fabrication of inorganic hollow and hollow core/shell materials with nanometer to micrometer dimensions have attracted considerable interest due to the materials' wide potential applications in catalysis, separation, chemical reactor, and controlled delivery and release of various substances.[1−4] Core/shell materials consist of a core structural domain covered by a shell domain.[5] In comparison to heterogeneous core/shell nanostructures (two different kinds of materials for the core and the shell), the homogeneous core/shell nanostructures (the same material for both the core and the shell) are much more difficult to prepare.[4] Current challenges in the synthesis of hollow and hollow core/shell materials essentially involve controlling their crystalline structures, morphologies, and sizes. Several methods, such as template-sacrificial techniques,[6] Ostwald ripening,[7] Kirkendall effect,[8] oriented attachment,[9,10] and chemically induced self-transformation,[11] have been employed to fabricate various hollow spheres.

Boehmite is an aluminum oxyhydroxide, which is the main precursor for production of γ-Al_2O_3 used in catalysis, adsorption, coating technologies, and in the preparation of alumina-based materials.[12,13] Boehmite can also be used as an orthopedic or a dental material due to its biocompatibility.[14] Owing to its thermal, chemical, and mechanical stabilities as well as catalytic and textural properties well-suited for both catalysis and adsorption, preparation of γ-Al_2O_3 with high surface area, tailored porosity, and controlled morphology attracted the attention of many researchers.[13,15−19] However, well-crystallized boehmite usually gives γ-Al_2O_3 with low surface area, whereas in most cases, the boehmite used in catalysis (often called pseudoboehmite) is poorly crystallized, less ordered, and does not contain intercalated water in the structure.[20−22] Therefore, it is still a great challenge to develop simple and efficient strategies for the synthesis of boehmite with controlled physicochemical properties (crystallinity, morphology, textural properties, etc.).[23]

In comparison to hydrolysis of aluminum alkoxides and precipitation of inorganic aluminum salts, the hydrothermal route is usually used to achieve a fine control of boehmite crystallinity over a wide range of synthesis conditions.[24] Depending on the methods of synthesis, boehmite displays a variety of morphologies, such as nanoscale hollow spheres,[25] hydrotalcite-type structures,[26] nanorods,[27] nanowires,[28] flower-like,[29] nanofibers, and nanotubes.[30] Medium-crystallized boehmites with a surface area smaller than 100 m^2/g were hydrothermally precipitated from aluminum salt solutions using urea as a precipitating agent.[31] Boehmite architectures with hollow and self-encapsu-

* To whom correspondence should be addressed. E-mail: jiaguoyu@yahoo.com (J.Y.), jaroniec@kent.edu (M.J.).
[†] State Key Laboratory of Advanced Technology for Material Synthesis and Processing and School of Chemical Engineering.
[‡] Kent State University.

10.1021/jp904570z CCC: $40.75
Published on Web 07/08/2009

lated structures have been selectively precipitated using a quite complicated route, in which polystyrene-*block*-polyhydroxylethyl acrylate amphiphilic block copolymer was employed as a structure-directing agent or by a complex hydrothermal strategy involving an aluminum nitrate−ethanol−trisodium citrate−water system under strictly controlled conditions, at least 24 h at 200 °C.[32,33]

Recently, a facile strategy, involving self-transformation and hydrothermal crystallization, was employed for the preparation of hierarchically organized boehmite hollow spheres with a nanoflake-like surface using aluminum sulfate salt and urea as reaction precursors.[34] However, to the best of our knowledge, the controlled fabrication of complex micro- and nanostructures in the presence of sodium tartrate mediating agent has not been reported yet. Herein, we report a simple but effective method for direct preparation of various hollow core/shell and hollow boehmite microspheres using aluminum sulfate as a precursor and urea and sodium tartrate as precipitating and mediating agents, respectively. The as-prepared microspheres exhibited controlled crystallinity and high surface area, which may greatly facilitate their applications. Preliminary tests of these microspheres for removal of organic pollutants from water were positive, which makes them promising materials for environmental applications.

2. Experimental Section

2.1. Sample Preparation. All reagents are analytical grade supplied by Shanghai Chemical Reagent Ltd. (P. R. China) and used as received without further purification. In a typical synthesis, $Al_2(SO_4)_3 \cdot 18H_2O$ (0.007 mol), $CO(NH_2)_2$ (0.028 mol), and sodium tartrate (0.00035 mol) powders were dissolved in distilled water to form a mixed solution (70 mL) under vigorous stirring for 0.5 h. The solution was placed in a 100 mL autoclave with a Teflon liner. The autoclave was maintained at 165 °C for 3 h and then air-cooled to room temperature. The white precipitate was collected and washed with distilled water and anhydrous alcohol several times. The final product was dried in a vacuum oven at 80 °C for 12 h. Similar experiments were performed by varying concentrations of sodium tartrate (C_{ST}) from 0 to 0.025 M and reaction times from 0.5 to 6.0 h at C_{ST} = 0.01 M and 165 °C.

2.2. Characterization. The X-ray diffraction (XRD) measurements, which were used to characterize the crystalline phase and crystallite size of the boehmite powders, were carried out by a Rigaku D/Max-RB diffractometer using Cu Kα radiation at a scan rate (2θ) of 0.05° s^{-1}. The accelerating voltage and applied current were 40 kV and 80 mA, respectively. The crystallite size of boehmite nanoparticles was quantitatively calculated using the Scherrer formula ($d = (0.9\lambda)/(B\cos\theta)$, where d, λ, B, and θ are crystallite size, Cu Kα wavelength (0.15418 nm), full width at half-maximum intensity (fwhm) of (020) peak in radians, and Bragg's diffraction angle, respectively).[35] Morphological analysis was performed by an S-4800 field emission scanning electron microscope (FE-SEM, Hitachi, Japan) with an acceleration voltage of 5 kV. Partially powdered samples were also ultrasonically dispersed in ethanol solution and then transferred onto a copper grid covered with carbon film for transmission electron microscopy (TEM) analysis performed on a JEM-2100F electron microscope (JEOL, Japan) at an accelerating voltage of 200 kV. Nitrogen adsorption isotherms were measured on a Micromeritics ASAP 2020 adsorption analyzer (USA). All as-prepared samples were degassed at 150 °C prior to adsorption measurements. The Brunauer−Emmett−Teller (BET) specific surface areas (S_{BET}) for the samples studied were calculated from nitrogen adsorption data in the relative pressure (P/P_0) range of 0.05−0.2. The single-point pore volumes were obtained by converting the amount adsorbed at the relative pressure of 0.99 to the volume of liquid nitrogen. Pore-size distributions (PSDs) for the low-surface-area (large pore) samples prepared without and with 0.0005 M sodium tartrate were determined from adsorption branches of nitrogen adsorption−desorption isotherms using the original Barret−Joyner−Halender (BJH) method.[36] For high-surface-area microspheres, which possessed smaller mesopores, the original BJH method underestimates pore sizes;[37] therefore, its modified version reported by Kruk, Jaroniec, and Sayari (KJS)[37,38] was applied.

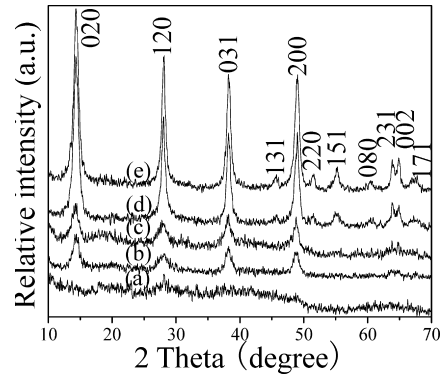

Figure 1. XRD patterns of the samples prepared by varying C_{ST} at 165 °C for 3 h: (a) 0.025, (b) 0.01, (c) 0.005, (d) 0.0005, and (e) 0 M.

2.3. Adsorption Experiments for Selected Organic Pollutants. Adsorption measurements for selected organic pollutants were performed by adding (under stirring conditions) 80 mg of as-prepared samples into 100 mL of Congo red ($C_{32}H_{22}N_6O_6S_2Na_2$) or phenol solutions having a concentration of 90 mg/L. Analytical samples were taken from the suspension after various adsorption times and separated by a microfiltration membrane. The Congo red and phenol concentrations were analyzed using a UV−vis spectrophotometer (UV-2550, Shimadzu, Japan). The same experiments were performed on commercial boehmite material that was obtained from the Research Institute of Petroleum Processing, China Petroleum Chemical Co., Ltd.

3. Results and Discussion

3.1. Structural Properties. Powder XRD was used to monitor the changes in the phase structure and crystallite sizes of the as-prepared samples. Figure 1 shows the wide-angle XRD patterns of the samples obtained by varying C_{ST} from 0.025 to 0 M. As can be seen from Figure 1, pattern a, there are no distinct diffraction peaks, which indicates the amorphous nature of the sample at C_{ST} = 0.025 M. For the samples obtained at smaller values of C_{ST} (0.01−0.005 M), all the diffraction peaks are in good agreement with those of the orthorhombic boehmite with lattice constants a = 3.69 Å, b = 12.24 Å, and c = 2.86 Å (JCPDS Card No. 21-1307). Broad diffraction peaks reveal the nanosize nature of these samples, indicating their poor crystallinity and high water content.[39] Further reduction of C_{ST} to 0.0005−0 M resulted in the substantial enlargement of intensity and significant reduction of dispersion of all boehmite XRD peaks, indicating an increase in the degree of crystallization and enlargement of crystallite sizes. Table 1 contains the average size of crystallites and relative crystallinity of the samples prepared at different C_{ST}. The relative crystallinity of

TABLE 1: Effects of C_{ST} on the Crystalline Size, BET Surface Area, and Pore Characteristics of the Samples Obtained at 165 °C for 3 h and the Sample Regenerated at 280 °C for 4 h

sample	C_{ST} (M)	crystalline size (nm)[a]	relative crystallinity[a]	S_{BET} (m^2/g)	pore volume (cm^3/g)	average pore size (nm)
a	0.025	–	–	412	0.36	3.7
b	0.01	6.4	1.00	269	0.47	8.1
c	0.005	7.1	1.11	200	0.46	11.7
d	0.0005	13.5	2.11	91	0.35	31.7
e	0	15.0	2.34	71	0.34	31.6
br[b]	0.01	7.7	1.20	215	0.35	8.2

[a] A (-) indicates no data because of the amorphous nature of the phase. [b] br, the boehmite sample obtained by regeneration of the sample b (C_{ST} = 0.01 M) after the second cycle.

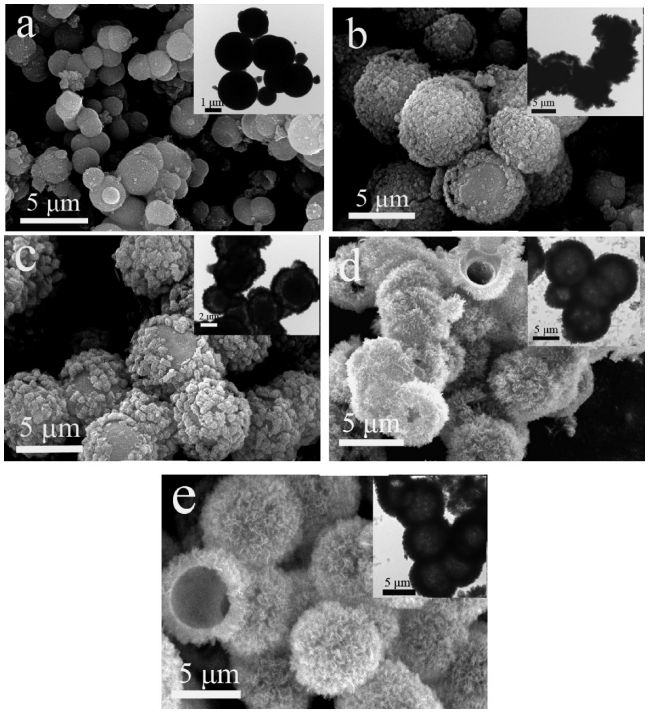

Figure 2. SEM and TEM images of samples prepared by varying C_{ST} at 165 °C for 3 h: (a) 0.025, (b) 0.01, (c) 0.005, (d) 0.0005, and (e) 0 M. The insets show the corresponding TEM images.

the sample prepared at C_{ST} = 0.01 M is assumed to be 1.00. The relative crystallinity of other samples is expressed as the ratio of its crystalline size to that of the sample prepared at C_{ST} = 0.01 M. As can be seen from this table, the aforementioned quantities increase with decreasing C_{ST}. Therefore, the addition of an appropriate amount of sodium tartrate facilitates, to some extent, the formation of boehmite microspheres with controlled crystallinity, but excess of this agent may lead to amorphous aluminum oxyhydroxide. Furthermore, no characteristic peaks from other crystalline impurities are present in Figure 1, indicating high purity of the resulting boehmite microspheres.

3.2. Morphology. The morphology and microstructure of the samples were further investigated by SEM and TEM. Figure 2 shows the SEM and TEM images (inset) of the samples prepared at different concentrations of sodium tartrate. As can be observed from Figure 2a, the amorphous aluminum oxyhydroxide spheres with diameters smaller than 3.0 μm were obtained for C_{ST} = 0.025 M. A decrease of C_{ST} to 0.01 M resulted in microspheres having some circular empty space between the core and shell, and these microspheres turned to hollow core/shell structures with diameters of ca. 2−5 μm (Figure 2b and its inset). The

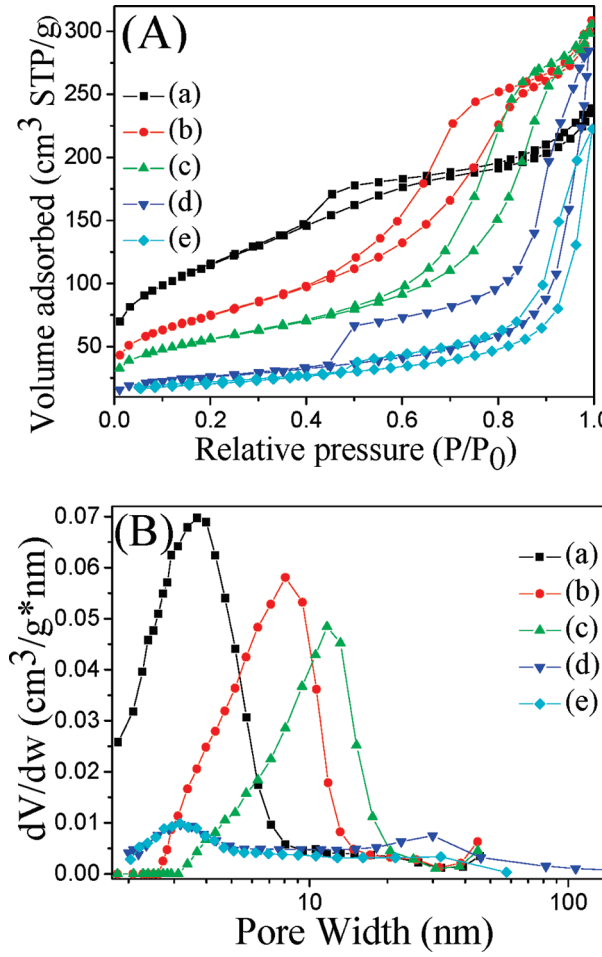

Figure 3. Nitrogen adsorption−desorption isotherms (A) and the corresponding pore-size distributions (B) of the samples prepared by varying C_{ST} at 165 °C for 3 h: (a) 0.025, (b) 0.01, (c) 0.005, (d) 0.0005, and (e) 0 M.

complex shells were formed by self-assembly of nanoflakes, which resulted in the partial ordering of loosely connected flakes. A further decrease of C_{ST} to 0.005 M led to microspheres in which the circular empty space between the core and shell was remarkably enlarged (Figure 2c and its inset), indicating the formation of the well-defined hollow core/shell microspheres. Finally, when C_{ST} approaches 0.0005 M, the microsphere cores disappeared completely and the urchin-like hollow microspheres with densely organized nanoflakes were formed with diameters of ca. 3−6 μm (Figure 2d,e and insets).

3.3. Surface Area and Porosity of Microspheres. The effect of C_{ST} on the pore structure and the BET surface area of boehmite microspheres was analyzed on the basis of nitrogen adsorption isotherms shown in Figure 3. As can be seen from Figure 3A, curve a, the amorphous microspheres obtained at C_{ST} = 0.025 M display a type IV isotherm according to the IUPAC classification.[40] This sample shows highest adsorption in the range of relative pressures below 0.4 P/P_0 among all samples studied, indicating high surface area. A small H2-type[40] hysteresis loop is observed in the range of 0.4−0.7 P/P_0, which closes at ~0.4 P/P_0, suggesting the presence of ink-bottle mesopores and/or pore constrictions. However, this hysteresis loop at the P/P_0 range of 0.8−1.0 resembles type H3, which may be associated with slitlike pores. Thus, two types of pores are possible: pores formed between agglomerated primary crystallites and pores between aggregated secondary particles.[40,41] Therefore, the corresponding pore-size distribution shown in

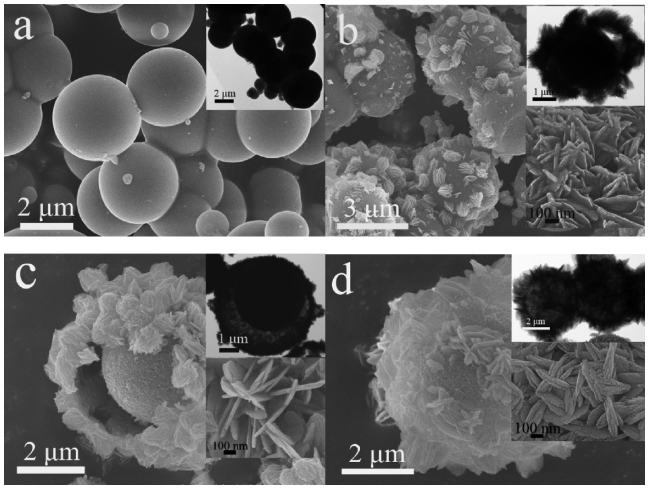

Figure 4. SEM and TEM images of the samples prepared at different reaction stages at $C_{ST} = 0.01$ M and 165 °C for (a) 0.5 h, (b) 1.0 h, (c) 3.0 h, and (d) 6.0 h.

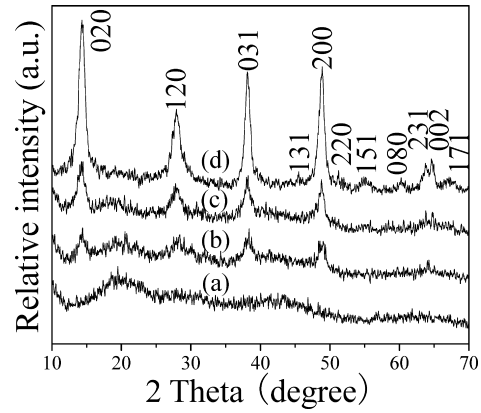

Figure 5. XRD patterns of the samples prepared at different reaction stages at $C_{ST} = 0.01$ M and 165 °C for (a) 0.5 h, (b) 1.0 h, (c) 3.0 h, and (d) 6.0 h.

Figure 3B is relatively broad and located at ~3.7 nm, indicating the presence of small and larger mesopores. A decrease of C_{ST} from 0.01 to 0 M caused a gradual change in the shape of adsorption isotherms and the corresponding pore-size distributions, implying a significant variation of pore structures. First, adsorption at the relative pressures below 0.4 P/P_0 decreased due to the surface area reduction caused by gradual disappearance of the amorphous phase. Second, the hysteresis loops become larger and are shifted significantly toward higher P/P_0, indicating larger mesopores. Third, the corresponding pore-size distributions become broader and are shifted in the direction of larger mesopores with decreasing C_{ST} (see the values of the pore width in Table 1). The aforementioned changes reflect a gradual transformation of amorphous aluminum oxyhydroxide into the hollow core/shell and hollow microspheres with higher crystallinity.

Table 1 contains the textural parameters of the as-prepared microspheres. As can be seen, the effect of sodium tartrate on the pore structure and the BET surface area of the microspheres studied is highly dependent on its concentration. The pore width increases with decreasing C_{ST} due to the growth of crystallites; simultaneously, the specific surface area and the pore volume decrease, except for the pore volume of the amorphous microspheres prepared at $C_{ST} = 0.025$ M. Boehmite microspheres with a large S_{BET} value of 269.0 m^2/g and the biggest pore volume of 0.47 cm^3/g were obtained at $C_{ST} = 0.01$ M. In comparison to solid particles of similar size, these porous boehmite hollow core/shell and hollow microspheres obtained at C_{ST} between 0.0005 and 0.01 M possess both the outer and the interior void space, which can be used to accommodate a large amount of guest molecules or large-size species. These structural features of the boehmite microspheres studied make them attractive for catalysis, adsorption, and biomedical applications, such as drug delivery and controlled storage/release of guest molecules.[42,43]

3.4. Possible Mediation Mechanism of Sodium Tartrate. To further investigate the effect of sodium tartrate on the formation of hollow core/shell and hollow microspheres, the time-dependent experiments were also carried out at $C_{ST} = 0.01$ M. After 0.5 h, amorphous solid aluminum oxyhydroxide microspheres with diameters of ca. 1−3 μm (Figures 4a and 5, pattern a) begin to appear. An increase in the reaction time to 1.0 h initiated the dissolution process at the regions near the surface of solid spheres (see inset in Figure 4b), and thus, the boehmite hollow core/shell microspheres started to form slowly by assembly of nanoflakes (Figure 4b and its inset). A further increase of the reaction time to 3.0 h resulted in the formation of a unique boehmite sphere-in-sphere superstructure with a gradually reduced size of the inner sphere having the urchin-like outer surface (Figures 4c and 5, pattern c). The outer surface consisted of a large quantity of orderly aggregated nanoplatelets with a thickness of ca. 20 nm (see inset in Figure 4c). A subsequent increase of reaction time to 6.0 h caused a complete dissolution of the inner solid sphere, resulting in a spiny-like boehmite hollow microsphere (Figures 4d and 5, pattern d). Moreover, the aggregated nanoplatelets on the surface became loose and their thickness increased to ca. 25 nm (see inset in Figure 4d). A broad width of the diffraction peaks (Figure 5, patterns b−d) also suggests that the crystals in these samples are in nanometer range. The estimation of the crystallite sizes by the Scherrer equation gave values of 6.3, 7.1, and 13.8 nm, respectively.

On the basis of the above experiments, a possible two-step growth mechanism of sodium tartrate-mediated self-transformation of metastable amorphous aluminum oxyhydroxide particles and their subsequent self-assembly into hollow core/shell and hollow microspheres with randomly aggregated nanoflakes is proposed. In the absence of sodium tartrate, Al^{3+} and urea can alternatively hydrolyze and polycondense, which leads to the precipitation of amorphous aluminum oxyhydroxide spheres promoted by sulfate anions.[44−47] An increase of reaction time facilitates transformation of the surface layer to thermodynamically more stable boehmite, as the supersaturation drops in the surrounding solution. Consequently, an ultrathin and less-soluble shell is formed via secondary nucleation and subsequent growth of boehmite crystal nuclei until the system reaches equilibrium with the surrounding solution.[7,48−51] Because boehmite has a distinctly $Al(O,OH)_6$ octahedral layered structure with plenty of surface-located hydroxyl groups, its nuclei growth may be afforded via hydrogen bonds along a preferential direction with the lowest growth energy.[52−54] Thus, the hydrogen bond-induced orientation of the neighboring boehmite nuclei can effectively direct them to grow into nanoflakes on the shell surface under suitable reaction conditions. Furthermore, a gradual release of micrometer/nanometer NH_3 and CO_2 bubbles due to the alternate hydrolysis of urea and Al^{3+} and a gas−liquid equilibrium in the autoclave may also play important role in the formation of the core/shell and hollow microspheres.[4,55−57]

As a complexing agent, tartrate ion consists of two planar halves, each of them a having carboxyl group, tetrahedral

carbon, and hydroxyl oxygen atom. These two halves are oriented in such a manner that the four carbon atoms lie in a plane.[58,59]After addition of sodium tartrate, its anion can coordinate Al^{3+} to form a tartrate−aluminum complex anion, which may prevent Al^{3+} polymerization.[60] Next, porous amorphous aluminum oxyhydroxide particles can selectively adsorb tartrate anions, resulting in the formation of hydrogen bonds between carboxyl and hydroxyl groups of tartrate ions and the surface OH groups of aluminum oxyhydroxide. The adsorbed tartrate anions, which are negatively charged, may also weaken the positive charge distribution on the primary particles and cause the shift in the isoelectric point of alumina.[61] As a result, not only the formation of well-defined amorphous aluminum oxyhydroxide spheres but also their subsequent transformation into crystallized boehmite and further self-assembly into boehmite hollow core/shell and hollow microspheres with randomly aggregated nanoflake-like surface can be reduced to some extent. This reduction trend can be gradually strengthened with increasing C_{ST}, resulting in smaller crystallinity of boehmite microspheres. Correspondingly, the structural evolution from hollow and hollow core/shell microspheres to almost completely solid microspheres is observed for boehmite, which transforms to amorphous aluminum oxyhydroxide at $C_{ST} = 0.025$ M. In usual cases of chemically induced self-transformation, the transformation from amorphous interior solid to hollow architecture was promoted by simple inorganic anions and surfactants in the solution.[11,33,48−51] However, in this case, sodium tartrate plays an opposite role under the reaction conditions studied. Nevertheless, a deeper investigation is needed to better understand the exact effect of sodium tartrate on the transformation of amorphous aluminum oxyhydroxide and its assembly into boehmite hollow core/shell and hollow microspheres with controlled structural and morphological properties.

3.5. Application in Wastewater Treatment. It was shown elsewhere[33,62−65] that hollow micro/nanostructured materials may possess desirable adsorption properties for removal of pollutants from water. To comparatively evaluate the potential application of the microspheres prepared with and without sodium tartrate, their adsorption capacities for organic pollutants from water were investigated at room temperature. Congo red, which is a common azo dye in textile industry, and phenol, which is a highly toxic organic compound in the wastewater after coal carbonization, were chosen as model pollutants. The characteristic absorptions of Congo red around 500 nm and phenol around 285 nm were chosen to monitor the adsorption process, and C/C_0 was used to characterize the relative adsorption capacity (C_0 and C represent the initial concentration and concentration after treatment, respectively). The effect of C_{ST} on the adsorption rate of Congo red is shown in Figure 6. As can be seen from this figure, an increase of C_{ST} from 0 to 0.01 M resulted in larger adsorption rates, reaching the highest value during a 90 min time period for the microspheres prepared at $C_{ST} = 0.01$ M; this observation is confirmed by the photo and UV/vis absorption curves recorded at different times (see Figure 7a,b, respectively). The adsorption capacities were calculated to be 109.0−111.3 mg/g for the microspheres prepared at C_{ST} between 0.0005 and 0.01 M, 93.7 mg/g for the microspheres prepared without sodium tartrate, and 51.0 mg/g for the amorphous microspheres prepared at $C_{ST} = 0.025$ M under the same conditions. Thus, it is clear that the adsorption performance of crystalline microspheres can be enhanced by increasing C_{ST}. Meanwhile, the adsorption capacities of microspheres prepared at C_{ST} between 0.0005 and 0.01 M changed little with time, indicating their good stability. In contrast, the microspheres

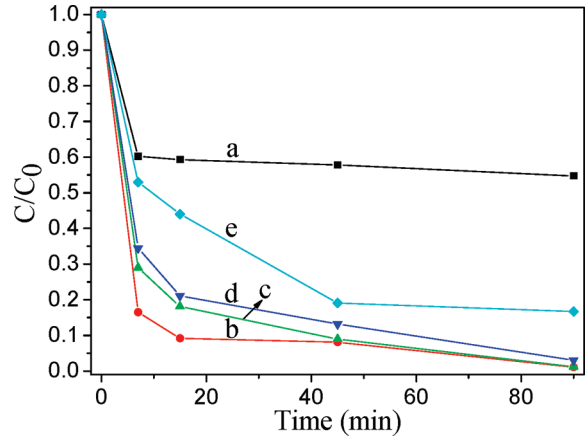

Figure 6. Adsorption rate of Congo red on the samples prepared by varying C_{ST}: (a) 0.025, (b) 0.01, (c) 0.005, (d) 0.0005, (e) 0 M.

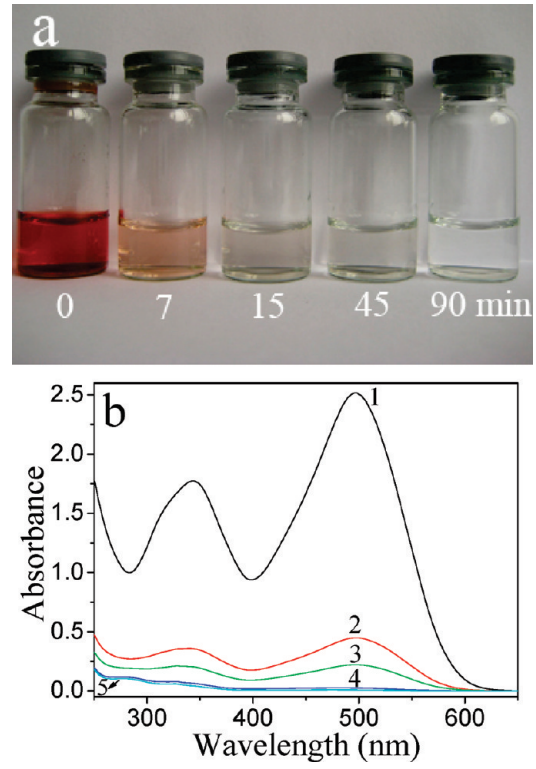

Figure 7. Picture of absorption of a Congo red solution with time (a) and the corresponding absorption spectra (b) in the presence of boehmite microspheres prepared at $C_{ST} = 0.01$ M after time intervals of (1) 0, (2) 7, (3) 15, (4) 45, and (5) 90 min.

prepared without sodium tartrate and the amorphous microspheres prepared at $C_{ST} = 0.025$ M showed much lower adsorption rates. The above results also suggest that phase structures of the samples obviously influence their adsorption performance and all boehmite samples have better adsorption performance than that of the amorphous sample. Another possible explanation is that the adsorption efficiency was facilitated to some extent by solvent entrapment and sequestration within the enclosed microspheres.[11] Furthermore, the boehmite microspheres containing Congo red could be regenerated by a simple thermal treatment in air at 280 °C for 4 h without diminishing their adsorption performance; their performance was even better after the second and third regeneration, as shown in Figure 8, curves a−c. The final removal ability of the regenerated material after four cycles was almost constant, as shown in Figure 8, curve d. Note that the regeneration of the

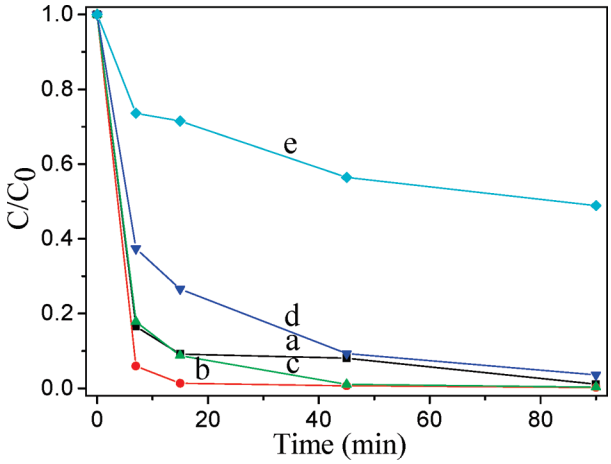

Figure 8. Adsorption rate of Congo red on boehmite microspheres prepared at $C_{ST} = 0.01$ M after the (a) first, (b) second, (c) third, and (d) fourth cycle and (e) for commercial boehmite.

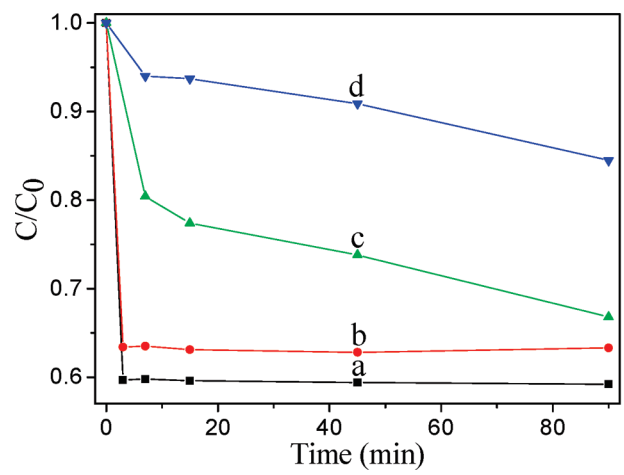

Figure 9. Adsorption rate of phenol on boehmite microspheres prepared at $C_{ST} = 0.01$ M after the (a) first and (b) second cycle, (c) for boehmite microspheres prepared without sodium tartrate, and (d) for commercial boehmite.

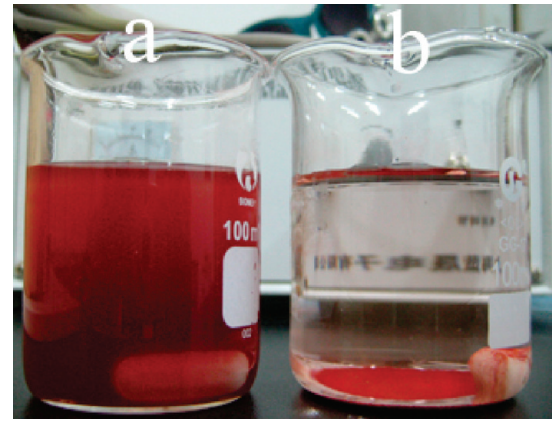

Figure 10. Picture of absorption of a Congo red solution on boehmite microspheres prepared at $C_{ST} = 0.01$ M after the second cycle (a) for a 90 min adsorption process and (b) after free sedimentation for 60 min.

boehmite sample prepared at $C_{ST} = 0.01$ M was performed at higher temperature (280 °C in air instead of 165 °C used in the hydrothermal synthesis of the initial sample), which resulted in about a 20% reduction of the surface area and pore volume, a slight enlargement of the pore width, and some improvement in crystallinity (see Table 1 and the Supporting Information, Figures S1and S2). This reduction of surface area did not decrease adsorption capacity of the microspheres toward Congo red; on the contrary, even some enhancement was observed due to activation of the boehmite surface, which may create more active sites at higher temperature. Moreover, the boehmite microspheres exhibited much higher adsorption efficiency than that of the commercial boehmite due to the unique hollow core/shell or hollow microstructure. The removal of Congo red may be associated with the electrostatic attraction and surface complexation via hydrogen bonding between the hydroxyl groups present on the surface of microspheres and amine groups of Congo red molecules.[64,66] The low pH value (≈6.0) of the original suspension also promoted the electrostatic attraction because the aluminum oxide surface was positively charged (isoelectric point of $Al_2O_3 \approx 9.0$). The discrepancies among the removal capacities of these microspheres could mainly result from the combination of several factors, such as phase structure, specific surface area, pore volume, and the unique core/shell structure. In addition, relatively narrow pore-size distributions with mesopores concentrated in the range of 8 to 12 nm for the samples prepared at C_{ST} between 0.005 and 0.01 M may also be an essential factor affecting adsorption affinity toward Congo red.

The removal capacities of the as-prepared boehmite microspheres and the commercial boehmite were further investigated by using phenol solution at pH = 8. Figure 9 shows that the hollow core/shell microspheres prepared at $C_{ST} = 0.01$ M exhibited the highest adsorption rate and reached the equilibrium removal capacity of 46.0 mg/g in a very short time of 3 min. In contrast, the removal capacities for the hollow microspheres prepared without sodium tartrate and for the commercial boehmite were only 37.4 and 17.4 mg/g after a long time period (90 min), respectively. The used hollow core/shell microspheres can also be regenerated by simply heating them in air at 350 °C for 2 h. Figure 9, curve b, shows the adsorption rate of phenol after the first regeneration of microspheres; the equilibrium removal capacity of 41.3 mg/g was achieved during a very short time of 3 min. A slight decrease in the removal capacity of the product and its facile regeneration suggest its promising applicability in water treatment. In addition, the solid/liquid separation may be easily achieved by a facile method such as sedimentation followed by filtration because of the relatively high density of boehmite microspheres containing organic pollutants and their micrometer sizes (Figure 10), which makes their usage feasible for large-scale applications. Thus, the present study provides a promising adsorbent for the application in organic wastewater treatment because of its facile preparation in large quantity, high removal capacity, and easy separation and regeneration.

4. Conclusions

A variety of boehmite hollow core/shell and hollow microspheres of good adsorption performance were prepared by a facile sodium tartrate-mediated hydrothermal process. The effect of sodium tartrate on the crystallinity, specific surface area, pore structure, and adsorption performance of boehmite microspheres is significant. A possible mediation mechanism of sodium tartrate involves the complexation ability and adsorption of tartrate anions, self-transformation of metastable amorphous aluminum oxyhydroxide particles, and subsequent self-assembly into boehmite hollow microspheres. An increase of sodium tartrate concentration at 165 °C for 3 h enhanced the aforementioned transformation,

resulting in the formation of amorphous aluminum oxyhydroxide at $C_{ST} = 0.025$ M. For C_{ST} between 0.0005 and 0.01 M, high-quality boehmite microspheres with a high specific surface area of 91.0−269.0 m^2/g and a pore volume of 0.35−0.47 cm^3/g were obtained and showed high adsorption affinity toward organic pollutants in water, which makes them promising for water treatment processes. The adsorption performance of all boehmite microspheres prepared with sodium tartrate was much higher than that of the boehmite microspheres prepared without sodium tartrate and that of commercial boehmite powder. Also, phase structures of the samples obviously influence their adsorption performance, and boehmite samples have better adsorption activity than that of the amorphous sample. The adsorption capacity of the hollow core/shell microspheres prepared at $C_{ST} = 0.01$ M with respect to Congo red and phenol reached the highest value of 111.3 and 46.0 mg/g, respectively; these microspheres were readily regenerated without diminishing their capacity. The positive effect of sodium tartrate, manifested by slowing crystallization and improving textural properties of microspheres at appropriate C_{ST}, seems to be the main factor causing the improvement of adsorption performance of boehmite hollow core/shell microspheres, suggesting that the adsorption efficiency was facilitated to some extent by solvent entrapment and sequestration within the enclosed microspheres. It is noteworthy that this synthesis strategy may be extended to the preparation of complex functional structures with controlled physicochemical properties for a variety of applications such as wastewater treatment.

Acknowledgment. This work was partially supported by the National Natural Science Foundation of China (50625208, 20773097, and 20877061), the China Postdoctoral Science Foundation project (20080440142), and the National Basic Research Program of China (2007CB613302 and 2009CB939704).

Supporting Information Available: A comparison of XRD patterns, nitrogen adsorption−desorption isotherms, and the corresponding pore-size distributions between the sample prepared at $C_{ST} = 0.01$ M at 165 °C for 3 h and its regenerated sample at 280 °C for 4 h after the second cycle. This material is available free of charge via the Internet at http://pubs.acs.org.

References and Notes

(1) Titirici, M.; Antonietti, M.; Thomas, A. *Chem. Mater.* **2006**, *18*, 3808.
(2) Chen, Z. T.; Gao, L. *Cryst. Growth Des.* **2008**, *8*, 460.
(3) Caruso, F.; Caruso, R. A.; Möhwald, H. *Science* **1998**, *282*, 1111.
(4) Cao, S. W.; Zhu, Y. J. *J. Phys. Chem. C* **2008**, *112*, 12149.
(5) Fleming, M. S.; Mandal, T. K.; Walt, D. R. *Chem. Mater.* **2001**, *13*, 2210.
(6) (a) Yu, J. G.; Yu, X. X.; Huang, B. B.; Zhang, X. Y.; Dai, Y. *Cryst. Growth Des.* **2009**, *9*, 1474. (b) Yu, J. G.; Yu, X. X. *Environ. Sci. Technol.* **2008**, *42*, 4902. (c) Yu, J. G.; Liu, W.; Yu, H. G. *Cryst. Growth Des.* **2008**, *8*, 930.
(7) Yu, H. G.; Yu, J. G.; Liu, S. W.; Mann, S. *Chem. Mater.* **2007**, *19*, 4327.
(8) Xie, L.; Zheng, J.; Liu, Y.; Li, Y.; Li, X. G. *Chem. Mater.* **2008**, *20*, 282.
(9) Teo, J. J.; Chang, Y.; Zeng, H. C. *Langmuir* **2006**, *22*, 7369.
(10) Zhang, Y. W.; Jiang, M.; Zhao, J. X.; Wang, Z. X.; Dou, H. J.; Chen, D. Y. *Langmuir* **2005**, *21*, 1531.
(11) Yu, J. G.; Yu, H. G.; Guo, H. T.; Li, M.; Mann, S. *Small* **2008**, *4*, 87.
(12) Feng, Y. L.; Lu, W. C.; Zhang, L. M.; Bao, X. H.; Yue, B. H.; Lv, Y.; Shang, X. F. *Cryst. Growth Des.* **2008**, *8*, 1426.
(13) Yuan, Q.; Yin, A. X.; Luo, C.; Sun, L. D.; Zhang, Y. W.; Duan, W. T.; Liu, H. C.; Yan, C. H. *J. Am. Chem. Soc.* **2008**, *130*, 3465.
(14) Webster, T. J.; Hellenmeyer, E. L.; Price, R. L. *Biomaterials* **2005**, *26*, 953.
(15) Park, H.; Yang, S. H.; Jun, Y.; Hong, W. H.; Kang, J. K. *Chem. Mater.* **2007**, *19*, 535.
(16) Cai, W. Q.; Li, H. Q.; Zhang, Y. *Mater. Chem. Phys.* **2006**, *96*, 136.
(17) (a) Cejka, J. *Appl. Catal., A* **2003**, *254*, 327. (b) Balcar, H.; Hamtil, R.; Zilkova, N.; Zhang, Z. R.; Pinnavaia, T. J.; Cejka, J. *Appl. Catal., A* **2007**, *320*, 56.
(18) (a) Pinnavaia, T. J.; Zhang, Z. R.; Hicks, R. W. *Stud. Surf. Sci. Catal.* **2005**, *156*, 1. (b) Jang, B.; Helleson, M.; Shi, C.; Rondinone, A.; Schwartz, V.; Liang, C. D.; Overbury, S. *Top. Catal.* **2008**, *49*, 145.
(19) Morris, S. M.; Fulvio, P. F.; Jaroniec, M. *J. Am. Chem. Soc.* **2008**, *130*, 15210.
(20) El-katatny, E. A.; Halawy, S. A.; Mohamed, M. A.; Zake, M. I. *J. Chem. Technol. Biotechnol.* **1998**, *72*, 320.
(21) Guzmán-Castillo, M. L.; Bokhimi, X.; Toledo-Antonio, A.; Salmones-Blásquez, J.; Hernández-Beltrán, F. *J. Phys. Chem. B* **2001**, *105*, 2099.
(22) Okada, K.; Nagashima, T.; Kameshima, Y.; Yasumori, A.; Tsukada, T. *J. Colloid Interface Sci.* **2002**, *253*, 308.
(23) Baumann, T. F.; Gash, A. E.; Chinn, S. C.; Sawvel, A. M.; Maxwell, R. S.; Satcher, J. H. *Chem. Mater.* **2005**, *17*, 395.
(24) Mathieu, Y.; Lebeau, B.; Valtchev, V. *Langmuir* **2007**, *23*, 9435.
(25) Buchold, D. H. M.; Feldmann, C. *Nano Lett.* **2007**, *7*, 3489.
(26) Benito, P.; Labajos, F. M.; Rives, V. *Cryst. Growth Des.* **2006**, *6*, 1961.
(27) He, T.; Xiang, L.; Zhu, S. *Langmuir* **2008**, *24*, 8284.
(28) Zhang, J.; Wei, S.; Lin, J.; Luo, J.; Liu, S.; Song, H.; Elawad, E.; Ding, X.; Gao, J.; Qi, S.; Tang, C. *J. Phys. Chem. B* **2006**, *110*, 21680.
(29) Zhang, J.; Liu, S.; Lin, J.; Song, H.; Luo, J.; Elssfah, E. M.; Ammar, E.; Huang, Y.; Ding, X.; Gao, J.; Qi, S.; Tang, C. *J. Phys. Chem. B* **2006**, *110*, 14249.
(30) Zhao, Y.; Frost, R. L.; Martens, W. N.; Zhu, H. Y. *Langmuir* **2007**, *23*, 9850.
(31) Mishra, D.; Anand, S.; Panda, R. K.; Das, R. P. *Mater. Lett.* **2002**, *53*, 133.
(32) Wu, X. Y.; Wang, D. B.; Hu, Z. S.; Gu, G. H. *Mater. Chem. Phys.* **2008**, *109*, 560.
(33) Zhang, L. M.; Lu, W. C.; Yan, L. M.; Feng, Y. L.; Bao, X. H.; Ni, J. P.; Shang, X. F.; Lv, Y. *Microporous Mesoporous Mater.* **2009**, *119*, 208.
(34) Cai, W. Q.; Yu, J. G.; Mann, S. *Microporous Mesoporous Mater.* **2009**, *122*, 42.
(35) Zhu, H. Y.; Gao, X. P.; Song, D. Y.; Bai, Y. Q.; Ringer, S. P.; Gao, Z.; Xi, Y. X.; Martens, W.; Riches, J. D.; Frost, R. L. *J. Phys. Chem. B* **2004**, *108*, 4245.
(36) Barrett, E. P.; Joyner, L. G.; Halenda, P. P. *J. Am. Chem. Soc.* **1951**, *73*, 373.
(37) Kruk, M.; Jaroniec, M.; Sayari, A. *Langmuir* **1997**, *13*, 6267.
(38) Kruk, M.; Jaroniec, M. *Chem. Mater.* **2001**, *13*, 3169.
(39) Bavykin, D. V.; Parmon, V. N.; Lapkin, A. A.; Walsh, F. C. *J. Mater. Chem.* **2004**, *14*, 3370.
(40) Sing, K. S. W.; Everett, D. H.; Haul, R. A. W.; Moscou, L.; Pierotti, R. A.; Rouquerol, J.; Siemieniewska, T. *Pure Appl. Chem.* **1985**, *57*, 603.
(41) (a) Yu, J. G.; Wang, G. H.; Cheng, B.; Zhou, M. H. *Appl. Catal., B* **2007**, *69*, 171. (b) Yu, J. G.; Wang, W. G.; Cheng, B.; Su, B. L. *J. Phys. Chem. C* **2009**, *113*, 6743.
(42) Lou, X. W.; Archer, L. A.; Yang, Z. C. *Adv. Mater.* **2008**, *20*, 4013.
(43) Fei, J. B.; Cui, Y.; Yan, X. H.; Qi, W.; Yang, Y.; Wang, K. W.; He, Q.; Li, J. B. *Adv. Mater.* **2008**, *20*, 452.
(44) Brosset, C.; Biedermann, G.; Sillén, L. G. *Acta Chem. Scand.* **1954**, *8*, 1917.
(45) Egon, M. *Acc. Chem. Res.* **1981**, *14*, 24.
(46) Maurizio, C.; Egon, M. *Chem. Mater.* **1989**, *1*, 78.
(47) Ramanathan, S.; Roy, S. K.; Bhat, R.; Upadhyaya, D. D.; Biswas, A. R. *Ceram. Int.* **1997**, *23*, 45.
(48) Yu, J. G.; Guo, H. T.; Davis, S. A.; Mann, S. *Adv. Funct. Mater.* **2006**, *16*, 2035.
(49) Wang, W. S.; Zhen, L.; Xu, C. Y.; Zhang, B. Y.; Shao, W. Z. *J. Phys. Chem. B* **2006**, *110*, 23154.
(50) Yu, J. G.; Liu, S. W.; Yu, H. G. *J. Catal.* **2007**, *249*, 59.
(51) Yu, J. G.; Liu, S. W.; Zhou, M. H. *J. Phys. Chem. C* **2008**, *112*, 2050.
(52) Penn, R. L.; Banfield, J. F. *Science* **1998**, *281*, 5379.
(53) Krokidis, X.; Raybaud, P.; Gobichon, A. E.; Rebours, B.; Euzen, P.; Toulhoat, H. *J. Phys. Chem. B* **2001**, *105*, 5121.
(54) Bokhimi, X.; Toledo-Antonio, J. A.; Guzman-Castillo, M. L.; Mar-Mar, B.; Hernandez-Beltran, F.; Navarrete, J. *J. Solid State Chem.* **2001**, *161*, 319.
(55) Zhang, Y. J.; Hu, Q. X.; Fang, Z. Y.; Cheng, T.; Han, K. D.; Yang, X. Z. *Chem. Lett.* **2006**, *35*, 944.
(56) Wang, X. J.; Wan, F. Q.; Gao, Y. J.; Liu, J.; Jiang, K. *J. Cryst. Growth* **2008**, *310*, 2569.

(57) Lin, F. Q.; Dong, W. S.; Liu, C. L.; Liu, Z. T.; Li, M. Y. *J. Colloid Interface Sci.* **2008**, *323*, 365.
(58) Ambady, G. K.; Kartha, G. *Acta Crystallogr., Sect. B* **1968**, *24*, 1540.
(59) Abdel-kader, M. M.; El-kabbany, F.; Taha, S. *J. Mater. Sci.: Mater. Electron.* **1990**, *1*, 201.
(60) Desroches, S.; Daydé, S.; Berthon, G. *J. Inorg. Biochem.* **2000**, *81*, 311.
(61) Palmqvist, L.; Lyckfeldt, O.; Carlström, E.; Davoust, P.; Kauppi, A.; Holmberg, K. *Colloids Surf., A* **2006**, *274*, 100.
(62) Fei, J. B.; Cui, Y.; Yan, X. H.; Qi, W.; Yang, Y.; Wang, K. W.; He, Q.; Li, J. B. *Adv. Mater.* **2008**, *20*, 452.
(63) Cao, S. W.; Zhu, Y. J. *J. Phys. Chem. C* **2008**, *112*, 6253.
(64) Yu, C. C.; Dong, X. P.; Guo, L. M.; Li, J. T.; Qin, F.; Zhang, L. X.; Shi, J. L.; Yan, D. S. *J. Phys. Chem. C* **2008**, *112*, 13378.
(65) Zeng, S. Y.; Tang, K. B.; Li, T. W.; Liang, Z. H.; Wang, D.; Wang, Y. K.; Zhou, W. W. *J. Phys. Chem. C* **2007**, *111*, 10217.
(66) Roth, W. J. *Pol. J. Chem.* **2006**, *80*, 703.

JP904570Z